Frequency conversion of femtosecond laser pulses in an engineered aperiodic poled optical superlattice

Yan Kong, Xianfeng Chen,* and Yuxing Xia

Department of Physics, The State Key Laboratory on Fiber Optic Local Area Communication Networks and Advanced Optical Communication Systems, Shanghai Jiao Tong University, 800 Dongchuan Road, Shanghai 200240, China

*Corresponding author: xfchen@sjtu.edu.cn

Received 28 March 2007; revised 14 May 2007; accepted 15 May 2007;
posted 15 May 2007 (Doc. ID 81571); published 8 August 2007

We theoretically propose a procedure based on a cascading genetic algorithm for the design of aperiodically quasi-phase-matched gratings for frequency conversion of optical ultrafast pulses during difference-frequency generation. By designing the sequence of a domain inversion grating, different wavelengths at the output idler pulse almost have the same phase response, so femtosecond laser pulses at wavelength 800 nm can be shifted to other wavelengths without group-velocity mismatch. © 2007 Optical Society of America

OCIS codes: 320.0320, 190.2620, 320.7090.

1. Introduction

Frequency conversion of a femtosecond pulse to another wavelength is significantly important in the widespread field of laser science and technology [1–3]. Femtosecond lasers have a wavelength bandwidth as large as tens of nanometers, and a temporal walk-off effect occurs as a result of large group-velocity mismatch (GVM). Only thin nonlinear crystal (approximately 100 μm thick) can be used for femtosecond laser frequency conversion. To meet the bandwidth and reduce the temporal walk-off effect, a 100 μm thick beta barium borate (BBO) crystal is often utilized for second-harmonic generation (SHG) of a femtosecond Ti:sapphire laser [4]. Unfortunately, the conversion efficiency is low due to the short length of the crystal. How to improve conversion efficiency and avoid GVM during a nonlinear parametric process remains a challenge. With the emergence of a domain reversal optical superlattice, a converted laser pulse can be compressed from a chirped femtosecond laser through a nonlinear parametric process, which is similar to chirped parametric amplification for generation of a high-power laser. The utility of the linearly and nonlinearly chirped gratings in quasi-phase matching for pulse compression and shaping by SHG has been demonstrated [5–9]. This technique relies on the engineering ability of quasi-phase-matched (QPM) gratings and allows compression of pulses at half of the wavelength of seed pulses. In the experiments reported in Refs. [5]–[9], unavoidable sum-frequency mixing occurred during SHG of femtosecond lasers. In addition, discrete domain reversal gratings were used for SHG because of the difficulty to fabricate continuous chirped gratings. As a result, much spectra were not used for pulse compression. To overcome this problem, a new procedure of designing aperiodically QPM gratings to compress an optical ultrashort pulse during SHG was reported previously [10]. In this method, the length of the domain block is fixed and can be selected artificially, so the difficulty of poling can be alleviated in comparison with that of chirped domain inversion gratings. Furthermore, this method can be used with the input fundamental pulse with arbitrary amplitude and phase. However, GVM between the fundamental and the SH pulse is still unavoidable, and the length of the crystal should be restricted to a few millimeters when the duration of the fundamental pulse is approximately hundreds of femtoseconds.

We extend this design to the sum-frequency generation (SFG) and difference-frequency generation (DFG) for wavelength shifts of optical ultrashort

0003-6935/07/235698-05$15.00/0

pulses. A continuous-wave laser with a sharp linewidth is employed together with a Ti:sapphire laser during the SFG or DFG process. Because SFG between two interactive pulses during SHG is avoided in this situation, the effect of GVM can be eliminated and the conversion efficiency can be significantly enhanced with a relatively long crystal. Frequency conversion of a femtosecond laser by DFG is discussed as an example.

QPM gratings generally use sign reversal of the nonlinear coefficient along the crystal length in a periodic or aperiodic fashion [10,11]; i.e., mathematically, $\mathrm{d}(z)$ is a square wave whose amplitude is the intrinsic nonlinear coefficient of the material d_{eff}. It can be decomposed into spatial Fourier components $\mathrm{d}_m(z)$ with slowly varying amplitudes and phase:

$$\mathrm{d}(z) = \sum_{m=-\infty}^{+\infty} \mathrm{d}_m(z) = \sum_{m=-\infty}^{+\infty} |\mathrm{d}_m(z)| \exp[iK_{0m}z + i\varphi_m(z)]. \tag{1}$$

We define a kind of grating that consists of a series of congruent nonlinear crystal blocks. The polarization direction of each block is determined by genetic algorithms. By applying this method we show how it is possible to design a QPM crystal that can be used to produce a near-transform–limited DFG pulse with a given wavelength.

2. Theories for Difference-Frequency Generation Pulse Compression in Quasi-Phase-Matched Gratings

The frequency-domain envelope $\hat{A}_m(z, \Omega_m)$ is defined as [6]

$$\hat{E}_m(z,\ \omega) = \hat{A}_m(z,\ \Omega_m)\exp[-ik(\omega_m + \Omega_m)z], \tag{2}$$

where the k vector is a function of frequency and $\Omega_m = \omega - \omega_m$ is the frequency detuning from the optical carrier angular frequency ω_m. We assume plane-wave interactions, the slowly varying envelope approximation, and the process of idler generation from the input signal and pump waves in the undepleted pump and unamplified signal approximation. (Here and in the remainder of the paper we use subscript $m = i, s, p$ to denote the idler, signal, and pump, respectively.) In terms of frequency-domain envelopes, we arrive at the following set of coupled-wave equations from Maxwell's equations in the frequency domain:

$$\frac{\partial}{\partial z}\hat{A}_i(z,\ \Omega_i) = -i\,\frac{\mu_0\omega_i^{\,2}}{2k_i}\,\hat{P}_{\mathrm{NL}}(z,\ \Omega_i)\exp[ik(\omega_i + \Omega_i)]z, \tag{3}$$

$$\frac{\partial}{\partial z}\hat{A}_s(z,\ \Omega_s) = 0, \tag{4}$$

$$\frac{\partial}{\partial z}\hat{A}_p(z,\ \Omega_p) = 0. \tag{5}$$

The nonlinear (NL) polarization is expressed as

$$\hat{P}_{\mathrm{NL}}(z,\ \Omega) = 2\varepsilon_0\mathrm{d}(z)\int_{-\infty}^{+\infty}\hat{A}_s^*(z,\ -\Omega + \Omega')\hat{A}_p(z,\ \Omega') \times \exp\{i[k(\omega_s - \Omega + \Omega') - k(\omega_p + \Omega')]z\}\mathrm{d}\Omega', \tag{6}$$

where we define $\Omega = \Omega_i = \omega - \omega_i$, $\Omega' = \omega' - \omega_p$, and use $\hat{A}_s^*(-\Omega) = \hat{A}_s^*(\Omega)$. From the Eqs. (3)–(6) we obtain the signal, pump, and the output idler envelope:

$$\hat{A}_s(z,\ \Omega) = \hat{A}_s(z = 0,\ \Omega) = \hat{A}_s(\Omega), \tag{7}$$

$$\hat{A}_p(z,\ \Omega) = \hat{A}_p(z = 0,\ \Omega) = \hat{A}_p(\Omega), \tag{8}$$

$$\hat{A}_i(L,\ \Omega) = -i\gamma\int_0^L \mathrm{d}(z)\mathrm{d}z\int_{-\infty}^{+\infty}\mathrm{d}\Omega'\hat{A}_s^*(\Omega' - \Omega)\hat{A}_p(\Omega') \times \exp[-i\Delta k(\Omega,\ \Omega')z], \tag{9}$$

where $\gamma = 2\pi/(\lambda_i n_i)$, λ_i is the idler wavelength, and n_i is the refractive index at the idler frequency and the k-vector mismatch:

$$\Delta k(\Omega,\ \Omega') = k(\omega_p + \Omega') - k(\omega_i + \Omega) - k(\omega_s + \Omega' - \Omega). \tag{10}$$

We now assume that the pump is a cw monochromatic wave, i.e., its frequency-domain envelope is a delta function [12],

$$\hat{A}_p(\Omega) = E_p\delta(\Omega = 0), \tag{11}$$

where E_p is the amplitude of the pump wave. Substituting Eq. (11) into Eq. (9) we obtain

$$\hat{A}_i(L,\ \Omega) = -i\gamma\hat{A}_s^*(-\Omega)E_p\int_{-\infty}^{+\infty}\mathrm{d}(z)\exp[-i\Delta k(\Omega)z]\mathrm{d}z, \tag{12}$$

where $\Delta k(\Omega)$ serves as the transform variable and is defined as

$$\Delta k(\Omega) = k(\omega_p) - k(\omega_i + \Omega) - k(\omega_s - \Omega). \tag{13}$$

The kind of grating that we defined consists of nonlinear crystal blocks, each with a length of l. Adjacent crystal blocks can have the same or the opposite nonlinear polarization direction. Figure 1 shows the ideal boundary position of the nth crystal block. But the ideal boundary departs from the original position, which could result from some typical but uncontrollable factors in the fabrication process. For example, in electric-field poled lithium niobate, Δl can be the uniformly overpoled or underpoled domain length at each domain boundary. In Section 3, we will

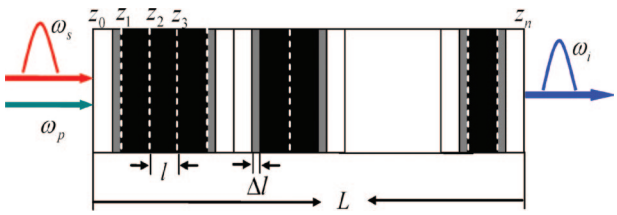

Fig. 1. (Color online) Schematic of pulse compression by DFG in aperiodically poled lithium niobate.

report on the influence of the overpoled domain at each domain boundary, when a cw pump beam and a prechirped femtosecond pulse are launched into an aperodically poled lithium niobate crystal. By optimizing the domain structure, the generated idler pulse has the same phase for different wavelengths. It is naturally expected that the idler pulse can be compressed.

3. Numerical Investigation and Discussion

We assume a cw monochromatic pump wave with optical carrier frequency ω_p and real (temporal peak) amplitude E_p, since its frequency-domain envelope can be represented as in Eq. (11). We also assume a linearly chirped Gaussian signal pulse whose optical carrier frequency is ω_s and whose real amplitude is E_s. The time-domain envelope of the electric field that corresponds to this pulse is

$$B_s(0,\ t) = E_s \frac{\tau_0}{\sqrt{\tau_0^2 + iC_1}} \exp\left[-\frac{t^2}{2(\tau_0^2 + iC_1)}\right]. \quad (14)$$

Using the frequency-domain envelope definition, we obtain $\hat{A}_s(\Omega)$ for this pulse as follows:

$$\hat{A}_s(\Omega) = \frac{1}{\sqrt{2\pi}} E_s \tau_0 \exp\left[-1/2(\tau_0^2 + iC_1)\Omega^2\right]. \quad (15)$$

According to Eq. (12), $\hat{A}_i(\Omega)$ is determined by the modulated nonlinear coefficient $d(z)$, crystal length L, and block numbers n. In our simulations, L and n are fixed, so our target is to determine the best distribution of the signs of the nonlinear coefficient so that the phase response is almost the same for all the frequency components of idler waves and will lead the output idler pulse to be compressed.

For the calculation we employed a cascading genetic algorithm to search for the best distribution of the sign of the nonlinear coefficient. To obtain a compressed idler pulse with a higher conversion efficiency and shorter pulse width, we should optimize the phase of the idler pulse. We chose a variance of different phases as the main objective function. The variance (which is the square of the standard deviation) can be described by

$$\sigma^2 = \frac{1}{n}\left[(\phi_1 - \bar{\phi})^2 + (\phi_2 - \bar{\phi})^2 + \cdots + (\phi_n - \bar{\phi})^2\right]. \quad (16)$$

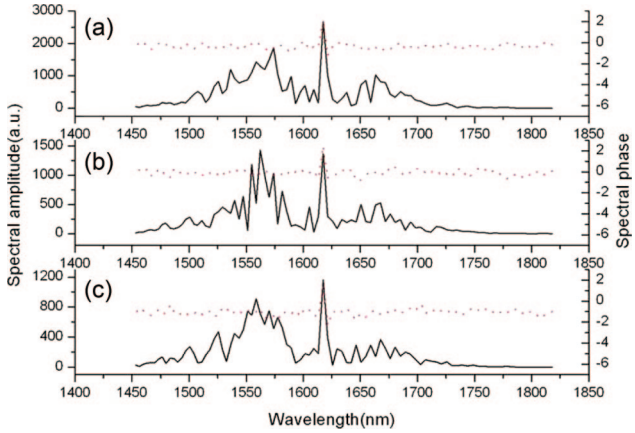

Fig. 2. (Color online) (a)–(c) Spectral amplitude (solid curve) and spectral phase (dotted curve) of the output idler pulse. The block lengths of the grating are 4, 5, and 8 μm.

In the simulations, the parameters of the input signal pulse are taken as $\tau_0 = 24.0$ fs (FWHM is 40.0 fs) and $C_1 = 20\tau_0^2$. The center wavelength of the signal pulse is 800 nm, the center wavelength of the pump pulse is 532 nm, the nonlinear optical crystal is lithium niobate, and temperature T is 25 °C. The refractive index of lithium niobate for different wavelengths was calculated from the Sellmeier data of Ref. [13]. The length of grating L was 5 mm; the length of each block l was chosen as 4, 5, and 8 μm, and $d(z)$ was optimized not only to make the phase response of the idler wave almost the same at the output, but also to make more frequencies meet QPM conditions.

Figure 2 shows the spectral amplitude and phase of the compressed idler pulse. After optimization of the domain inversion structure, the phase of the generated difference-frequency pulse became relatively uniform for the wavelengths from 1453 to 1818 nm. The calculated results also indicate that the efficiency increases with the decline of the block length. On the assumption that the generated idler pulse is still a Gaussian profile, the ideal full width at half-maximum (FWHM) duration for the transform-limited pulse is calculated to be 56.3 fs at a wavelength of 1588 nm. Our results, indicate that the calculated idler pulse durations (FWHM) are 35.4, 36.0, and 36.3 fs, which are less than the transform-limited value shown in Fig. 3. We note that the spectral amplitude is relatively irregular, not a Gaussian distribution, so the generated pulse can be even shorter than the Gaussian transform-limited pulse. It should be noted that, for pulse spectra from 1453 to 1818 nm, the ideal transform-limited pulse is approximately 24.8 fs. The duration of a generated pulse is still larger than an ideal transform-limited pulse because of phase and amplitude fluctuations. In addition, for fixed block length l, the longer the grating, the higher the conversion efficiency.

In the fabrication process, the poling error is introduced into the boundaries of each domain block. In our simulation when an error domain length is added to the boundary of a domain block, an equal amount

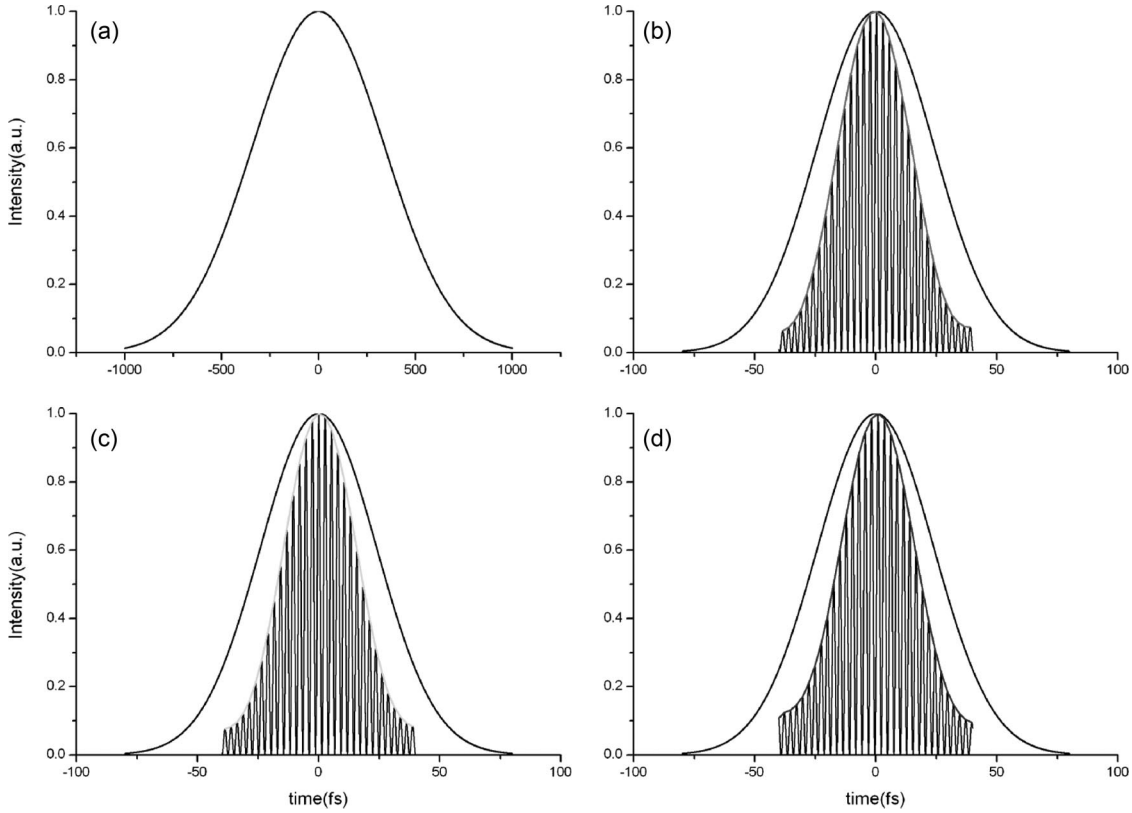

Fig. 3. (a) Input of the linearly chirped pulse intensity; (b)–(d) intensity of the DFG and the transform-limited pulse. The block lengths of the grating are 4, 5, and 8 μm. The pulse widths are 35.4, 36.0, and 36.3 fs.

of the length is subtracted from its adjacent domain block, as shown in Fig. 1. Figure 4 shows the simulation result for a grating that has overpoled domain errors of $\Delta l/l = 10\%$ and $\Delta l/l = 20\%$, and block length l of the grating is 5 μm. The error we set is reasonable by the current room temperature poling technology. With the simulations, it is obvious in Fig. 4 that the compressed pulse is highly insensitive to fabrication errors.

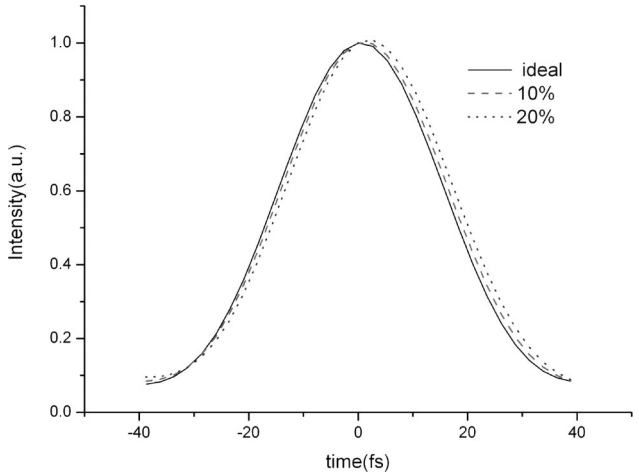

Fig. 4. Simulation result for the grating with overpoled domain errors of $\Delta l/l = 10\%$ (dash) and $\Delta l/l = 20\%$ (dot); the block length of the grating is 5 μm.

4. Conclusions

In conclusion, we have theoretically demonstrated an analytical approach to the design of a domain inversion grating that can compress idler waves during difference-frequency generation. A cascading genetic algorithm was used to optimize the distribution of the nonlinear coefficient of each block to make the phase response the same for frequencies within the spectra of the input pulse. In our simulation, the ultrafast pulse at the wavelength of 800 nm is shifted to 1580 nm by the DFG nonlinear process. We also simulated the influence of typical fabrication errors on the converted pulse and found that it is fairly insensitive.

This research was supported by the National Natural Science Foundation of China, grants 60477016 and 10574092; the National Basic Research Program 973 of China, 2006CB806000; and the Shu-Guang Scholar Plan of the Shanghai Education Committee.

References

1. S. Ashihara, T. Shimura, and K. Kuroda, "Group-velocity matched second-harmonic generation in tilted quasi-phase-matched gratings," J. Opt. Soc. Am. B **20,** 853–856 (2003).
2. N. Fujioka, S. Ashihara, H. Ono, T. Shimura, and K. Kuroda, "Group-velocity-matched noncollinear second-harmonic generation in quasi-phase matching," J. Opt. Soc. Am. B **22,** 1283–1289 (2005).
3. S.-M. Gao, C.-xi Yang, and G.-F. Jin, "Wavelength converter based on linearly chirped gratings in lithium niobate through

cascaded second-order processes," Chin. Phys. Lett. **20,** 1272–1274 (2003).
4. J.-y. Zhang, J. Y. Huang, H. Wang, K. S. Wong, and G. K. Wong, "Second-harmonic generation from regeneratively amplified femtosecond laser pulses in BBO and LBO crystals," J. Opt. Soc. Am. B **15,** 200–209 (1998).
5. M. A. Arbore, A. Galvanauskas, D. Harter, M. H. Chou, and M. M. Fejer, "Engineerable compression of ultrashort pulses by use of second-harmonic generation in chirped-period-poled lithium niobate," Opt. Lett. **22,** 1341–1343 (1997).
6. G. Imeshev, M. A. Arbore, M. M. Fejer, A. Galvanauskas, M. Fermann, and D. Harter, "Ultrashort-pulse second-harmonic generation with longitudinally nonuniform quasi-phase-matching gratings: pulse compression and shaping," J. Opt. Soc. Am. B **17,** 304–318 (2000).
7. G. Imeshev, M. A. Arbore, S. Kasriel, and M. M. Fejer, "Pulse shaping and compression by second-harmonic generation with quasi-phase-matching gratings in the presence of arbitrary dispersion," J. Opt. Soc. Am. B **17,** 1420–1437 (2000).
8. P. Loza-Alvarez, M. Ebrahimzadeh, W. Sibbett, D. T. Reid, D. Artigas, and M. Missey, "Femtosecond second-harmonic pulse compression in aperiodically poled lithium niobate: a systematic comparison of experiment and theory," J. Opt. Soc. Am. B **18,** 1212–1217 (2001).
9. U. Sapaev and D. T. Reid, "General second-harmonic pulse shaping in grating-engineered quasi-phase-matched nonlinear crystals," Opt. Express **13,** 3264–3276 (2005).
10. P. Li, X. Chen, Y. Chen, and Y. Xia, "Pulse compression during second-harmonic generation in engineered aperodic quasi-phase-matching gratings," Opt. Express **13,** 6807–6814 (2005).
11. X. Chen, F. Wu, X. Zeng, Y. Chen, Y. Xia, and Y. Chen, "Multiple quasi-phase-matching in a nonperiodic domain-inverted optical superlattice," Phys. Rev. A **69,** 013818 (2004).
12. G. Imeshev, M. M. Fejer, A. Galvanauskas, and D. Harter, "Pulse shaping by difference-frequency mixing with quasi-phase-matching gratings," J. Opt. Soc. Am. B **18,** 534–539 (2001).
13. D. H. Jundt, "Temperature-dependent Sellmeier equation for the index of refraction, *ne,* in congruent lithium niobate," Opt. Lett. **22,** 1553–1555 (1997).